Journal of Polymer Science

WILEY

JOURNAL OF POLYMER SCIENCE

RESEARCH ARTICLE OPEN ACCESS

The Copolymerization Performance of 2-Cyclopropyl-2-Oxazoline and 2-Cyclopropyl-2-Oxazine Contributes to Tunable Temperature-Responsive (Co) Polymer Characteristics

Katja P. Schumann[1] | Theresa M. Lutz[1] | Meike N. Leiske[1,2]

[1]Macromolecular Chemistry, University of Bayreuth, Bayreuth, Germany | [2]Bavarian Polymer Institute, Bayreuth, Germany

Correspondence: Meike N. Leiske (meike.leiske@uni-bayreuth.de)

Received: 17 December 2024 | **Revised:** 24 April 2025 | **Accepted:** 28 April 2025

Funding: This work was supported by the German Research Foundation (Grant 326998133 and 391977956).

Keywords: 2-oxazine | 2-oxazoline | cationic ring-opening polymerization | cloud point temperature | thermal properties

ABSTRACT

Even though the libraries of cyclic imino ethers, that is, 2-oxazoline and 2-oxazine monomers with different side chain substituents, have increased over the last years, there are still unsolved questions. Especially the less-studied kinetic properties, which are influenced by the nucleophilic potential of monomeric cyclic imino ethers interacting with terminal groups of growing polymer chains, are addressed. Here, the focus is on the kinetic principles governing 2-oxazolines and 2-oxazines with identical cyclopropyl side chains during homo- and copolymerization. We identified that the monomeric interaction with polymeric, terminal 2-oxazolinium species is favored over 2-oxazinium ions in both the homo- and cross-propagation. Moreover, temperature-dependent measurements in water–ethanol mixtures proved the upper critical solution temperature behavior of poly(2-cyclopropyl-2-oxazine)$_{25}$ compared to the 2-oxazoline-/2-oxazine-based variants of higher polymerization degree and copolymers, which possess lower critical solution temperature characteristics. The low glass transition temperature of poly-2-oxazines is increased by the co-synthesis with 2-oxazolines. This study provides information on the nucleophilic attack during the cationic ring-opening polymerization of 2-oxazolines and 2-oxazines and highlights how the combination of 2-cyclopropyl-2-oxazoline and 2-cyclopropyl-2-oxazine can be used to manipulate the temperature-dependent properties of the polymers.

1 | Introduction

In past decades, poly(cyclic imino ether)s (PCIEs) have gained attention for their chemical versatility and unique tailored properties [1–3]. Intriguingly, different side chains within PCIEs facilitate the formation of novel monomers with hydrophilic/hydrophobic, (un-)charged, and stimuli-responsive moieties for chemical and biological applications [4]. The polymerization of the five-membered 2-oxazolines *via* the cationic ring-opening polymerization (CROP) yielding poly(2-oxazoline)s (POx) was first reported in the 1960s [5–8] and since then, they have evolved as the most heavily researched member of this monomer family. Besides linear POx, the CROP synthesis strategy serves to create more sophisticated structures such as polymeric brushes, core cross-linked micelles, or hydrogels [9–13].

Since 2004, the simplest technique to generate monomers and (co)polymers has been the utilization of microwave technology,

The first two authors contributed equally to this study.

which has, in particular, fostered further research on functional POx. By now, various telechelic POx with functional α- and ω-groups have been synthesized by using functional initiators or termination agents, respectively [14]. Thus, the (co)polymerization of different 2-oxazoline monomers with varying substituents in 2-position enables further tuning of the polymer properties in a precise manner [15–17]. Moreover, detailed investigations in the polymerization kinetics of 2-oxazolines have provided a comprehensive overview of the parameters influencing the polymerizability of 2-oxazolines [18] and synthesis of homo- and heteropolymers [19]. In particular, variations of the polymerizable unit itself, the ring structure, have become a focus of research. Besides five-membered 2-oxazolines, six-membered 5,6-dihydro-4H-1,3-oxazines—which are commonly abbreviated as 2-oxazines in literature—as well as even seven-membered 2-oxazepines have been investigated regarding their polymerizability, either homopolymers or heteropolymers, as well as the properties of the resulting polymers [20]. Due to lowered ring tension and increased steric hindrance, the propagation rate constant (k_p) decreases in the following order: 2-oxazoline > 2-oxazine > 2-oxazepine [20], which affects the polymerization kinetics by reaction speed and favored monomeric attack. For example, previously reported copolymerization kinetics of 2-oxazolines and 2-oxazines revealed a reactivity switch due to end-group effects during the chain-growth [21, 22]. In this context, Hoogenboom and coworkers have investigated the copolymerization kinetics of different 2-oxazolines and 2-oxazines [21, 22]. Their results showed that compared to homopolymerizations, the rate constants of both 2-oxazoline and 2-oxazine are reduced. However, the higher nucleophilicity of 2-oxazines enables a faster attachment to the reactive 2-oxazolinium chain end and thus, an acceleration of the monomer consumption [23]. In the past, few studies have investigated the copolymerization kinetics of 2-oxazolines and 2-oxazines [21, 22]. Reportedly, the combination of an increased nucleophilicity of 2-oxazines and the decreased steric hindrance of 2-oxazoline-derived active chain ends facilitates significant acceleration of the propagation rate constant of 2-oxazines [22]. Previous studies have focused on the copolymerization of monomers with different side-chain substituents, which also knowingly impact the propagation rate constant [18]. Reports covering the copolymerization of hydrophilic 2-oxazolines and more hydrophobic 2-oxazines with identical substituents in the 2-position and the effect of variations concerning the monomer ratio on the reactivity of the individual monomers, as well as the solubility characteristics of those newly formed polymers, are rare and have to be addressed in more detail. One particularly interesting feature of different PCIEs is their temperature response in aqueous environments. Some polymers possess thermo-responsive behavior: lower critical solution temperature (LCST) and upper critical solution temperature (UCST) type polymers show a sharp coil to globule transition when the temperature exceeds (LCST) or decreases below (UCST) a temperature threshold. The most prominent example of an LCST type polymer is poly(*N*-isopropylacrylamide) [24], however, in recent years also PCIEs like POx and poly(2-oxazine)s (POz) have gained attention for the LCST behavior. In 2008, Hoogenboom *et al.* reported the dependency of LCST on molecular weight for poly(2-ethyl-2-oxazoline) and poly(2-*n*-propyl-2-oxazoline) [25]. Variations of the side chain also influence LCST, which was, for example, shown by Bloksma *et al.* for the three isomers of poly(2-propyl-2-oxazoline) [26]. Another way to tune the LCST is through copolymerization which was shown for linear and comb copolymers of 2-*iso*-propyl-oxazine and 2-methyl-2-oxazine by Warne *et al.* [27] among others [28–32]. Poly(2-cyclopropyl-2-oxazoline) is known for its applications in the biofabrication context, which are facilitated by its LCST properties [33]. Similar to LCST, the (co)polymer composition and concentration, as well as the solvent formulation are crucial influencing factors for UCST behavior [34, 35]. Supramolecular assembly by intra- and intermolecular interactions is favored by increasing hydrophobicity caused for example by alkyl chains and π-electron ring systems in the side chains of synthesized POx. Hence, the more pronounced the monomer side-chain hydrophobicity—for example, of 2-nonyl-2-oxazoline and 2-phenyl-2-oxazoline compared to 2-methyl-2-oxazoline and 2-ethyl-2-oxazoline—the more prone UCST behavior of the formed (co)polymers is [36]. Moreover, measurements with ethanol (EtOH)–water mixtures have shown that copolymers with stronger hydrophobic character require a higher concentration of EtOH to induce UCST response [36]. Further increasing the EtOH concentration leads to POx solubility, whereas an excess of H_2O results in POx insolubility as these water molecules form hydrate shells clustered around the EtOH molecules and are unable to interact with the POx [35]. Besides the polymeric and solvent factor, the UCST and LCST of a peptidomimetic polymer may be heavily influenced by the ionic strength as well as the type of solvated ions in an aqueous system [37, 38], which is of high relevance for any application in a biological environment. For example, Bloksma *et al.* studied the effect of different salts and various concentrations thereof on POx with varying hydrophobicity: the more hydrophilic the polymer the greater the effect of ions on the solubility [37]. The thermo-response and tailored hydrophilicity of PCIEs with tailored side-chain chemistry might be valuable for applications as polymeric additives in research concerning microplastics or the preparation of micro- and nanoparticles for biomedical applications. In particular, their hydrophilic–hydrophobic balance tailors them suitable to improve the hydrophilicity of hydrophobic materials, enabling an increase in interaction with biological matter such as enzymes, which can trigger the hydrolytic degradation of synthetic materials [39, 40].

The goal of this work was the comparison of hydrophilic 2-oxazolines and more hydrophobic 2-oxazines with cyclopropyl residues in the side chain: (i) the established 2-cyclopropyl-2-oxazoline (cPrOx) and (ii) the more scarcely reported 2-cyclopropyl-2-oxazine (cPrOz), as well as copolymerized, amphiphilic molecules thereof were assessed concerning the synthesis kinetics. In detail, we wanted to understand the effect of the nucleophilicity of the cyclic imino ether and the cyclopropyl substituent on the (co)polymerization of both monomers. Thus, we were interested in studying the effects of the ring chemistry exclusively and applied the monomers cPrOx and cPrOz, which feature identical substituents in the 2-position. In addition, we studied the thermal and solution properties of the formed (co)polymers with different polarity to gain further insights into the influence of monomer characteristics on the polymer properties such as solubility. In summary, the aim of the work is to gain insights into the synthesis kinetics of homo- and copolymerization combining five- and six-membered rings with similar substituents by CROP and investigate the comparative thermal properties, for

example, UCST and LCST material behavior in bulk and solution to address fundamental research questions that still hold in the literature.

2 | Results and Discussion

2.1 | Homopolymerization Kinetics

The two monomers of interest, cPrOz (Figure S1A–C) and cPrOx (Figure S1D), were synthesized according to literature procedures [26, 41]. Afterward, the homopolymerization kinetics of cPrOx and cPrOz were determined to confirm the living character of the polymerizations and to determine k_p of both monomers under identical polymerization conditions. The time-dependent conversion was analyzed by ^{1}H-NMR spectroscopy (Figures 1 and S2). Furthermore, the evolution of the molar mass and dispersity was analyzed with SEC (Figures 2 and S3).

For the first-order kinetic plot of cPrOx (Figure 1A), the signals at $\delta = 0.85$ ppm (4H) and $\delta = 4.17$ ppm were compared for the polymerization times from 0 to 900 s. Under the used reaction conditions, the polymerization proceeded in a controlled manner, as can be seen from the linear behavior of the kinetic plot. The increased standard deviation at higher monomer conversion (±15%) might be explained by increased sample viscosity and, hence, slightly altered propagation speed (Figure S2B). The determined $k_p = 0.19 \pm 0.04\ \mathrm{L\,mol^{-1}\,s^{-1}}$ for 2-cyclopropyl-2-oxazoline is in a similar range as the value previously reported by Goossens *et al.* ($k_p = 0.27 \pm 0.01\ \mathrm{L\,mol^{-1}\,s^{-1}}$) [42]. This study further reported the dependency of k_p on electrostatics by comparing k_p of the isomers 2-*n*-propyl-2-oxazoline ($k_p = 0.09 \pm 0.00\ \mathrm{L\,mol^{-1}\,s^{-1}}$) and 2-*iso*-propyl-2-oxazoline ($k_p = 0.05 \pm 0.01\ \mathrm{L\,mol^{-1}\,s^{-1}}$). It was suggested that the substituent in the 2-position influences the charge of the nitrogen atom, and therefore the nucleophilicity of the monomer. The experimental findings were previously confirmed by density functional theory (DFT)-calculations [42].

In this regard, we were keen on studying the polymerization kinetics of cPrOz (Figure 2B) to find out whether a similar effect might be observed for this monomer class, which is commonly polymerizing slower than its five-ring equivalents due to lower ring tension and higher steric hindrance [20].

For the first-order kinetic plot, the signals at $\delta = 0.75$ ppm (4H) and $\delta = 4.10$ ppm were compared for polymerization times from 0

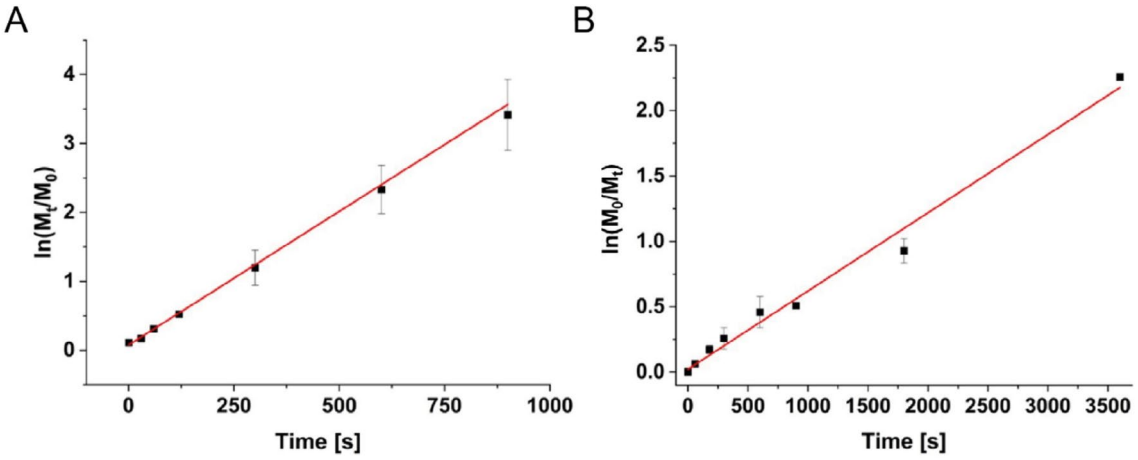

FIGURE 1 | First-order kinetic plot with standard deviation of cPrOx (A) and cPrOz (B). Reaction conditions: $T = 140$°C; $[M]/[I] = 100$; $M_0 = 2$ M; solvent: acetonitrile; initiator: methyl tosylate (MeOTos).

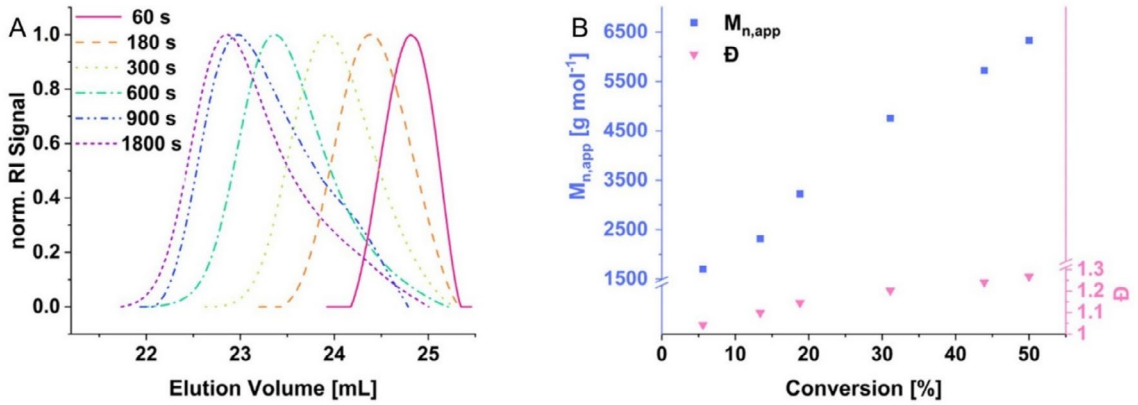

FIGURE 2 | Molar mass distribution (SEC in DMF, PS-cal.) of the homopolymerization kinetics of cPrOz. (A) SEC traces and (B) conversion-dependent development of $M_{n,app}$ and $Đ$. $T = 140$°C; $[M]/[I] = 100$; $M_0 = 2$ M; solvent: acetonitrile; initiator: MeOTos.

to 1800 s (Figure S2). Under the used reaction conditions (140°C; $[M]/[I] = 100$; $M_0 = 2$ M; solvent: acetonitrile and MeOTos as initiator), the polymerization proceeded in a controlled manner, as can be seen in the linear behavior of the kinetic plot. An issue that should be mentioned is that for the second kinetic, the samples for 1800 and 3600 s unexpectedly turned solid and yellow with clear supernatant. However, the solubility behavior of the formed polymer was unaffected and thus, the solid could be dissolved in organic solvents such as chloroform. In addition, we assessed an ^{1}H-NMR spectrum to address possible artifacts of side products. Owing to the absence of such pollutants, we analyzed the peak integration of the copolymerization product. As reported in the literature for PcPrOx, the problem with phase separation only occurs upon cooling [42]. The kinetics of cPrOz proceeded in a highly reproducible manner ($k_p = 0.029 \pm 0.002$ L mol^{-1} s^{-1}). The observed k_p value was compared to the isomers 2-*n*-propyl-2-oxazine ($k_p = 0.029 \pm 0.003$ L mol^{-1} s^{-1}) [43] by Bloksma *et al.* and 2-*iso*-propyl-2-oxazine ($k_p = 0.016$ L mol^{-1} s^{-1}) [27] by Kempe and coworkers. With the reactivities of the 2-propyl-2-oxazoline isomers in mind (as described above), it might be assumed that the same trend would be observed for the 2-propyl-2-oxazines. However, the determined propagation constant is identical to the propagation constant for 2-*n*-propyl-2-oxazine. It was concluded that the steric hindrance of the six-membered ring has a greater effect than the nucleophilicity of the side-chain functionality. The observed propagation rate constant for cPrOx ($k_p = 0.187 \pm 0.036$ L mol^{-1} s^{-1}) was approximately six times higher compared to cPrOz ($k_p = 0.029 \pm 0.002$ L mol^{-1} s^{-1}). The change in reactivity is in line with previously reported results and can be explained by lower ring tension and lack of planarity and therefore higher steric hindrance in the 2-oxazine [43].

For the kinetic of cPrOx neither fronting nor tailing was observed in SEC measurements (Figure S3A). At 100% conversion, a $Đ$ of ~1.5 was determined, which is comparable to $Đ$ reported in literature with similar reaction conditions [26]. For the $M_{n,app}$, a linear increase with increasing conversion was observed (Figure S3B). In comparison, for cPrOz and longer polymerization times, some tailing was observed in SEC (Figure 2A) indicating chain transfer or termination. This finding was further supported by the slight increase of $Đ$ up to 1.25 (50% conversion) (Figure 2B). For P(2-*n*-propyl-2-oxazine)$_{100}$, $Đ = 1.37$ was reported in 2012 by Bloksma *et al.* [43] which is slightly lower compared to our measurements. The deviation is likely due to higher X_n, as $Đ$ often increases with higher $[M]/[I]$ ratios [43]. For the $M_{n,app}$, a linear increase with progressing conversion was observed (Figure 2B) depending on the growing polymeric chain length.

2.2 | Copolymerization Kinetics

Copolymerization kinetics were conducted at monomer ratios ($[M]_{0,cPrOx}$:$[M]_{0,cPrOz}$) of 10:90, 25:75, 50:50, 75:25, and 90:10. The conversion was monitored via ^{1}H NMR measurements (Figure S4, Table S1). The derived plots (Figure 3A,B) revealed the expected exponential correlation of the kinetics [22], in contrast to the linear pseudo first-order kinetics observed for the homopolymerization of each monomer. Having a closer look at the monomer fraction in the polymer chain at varying monomer conversion (Figure 3C,D), it is obvious that at very low conversion (i.e., ≤5%), the fraction of cPrOz in the polymer chain is close to or even below the feed fraction of this monomer. In contrast, around 10% monomer conversion, a boost of the incorporated monomer fraction confirmed an acceleration of the propagation constant. The increase of the propagation speed was found to be more distinct at lower feed ratios of cPrOz. In addition, the maximum deviation of the monomer fraction from the feed ratios was also found to be dependent on the monomer feed ratio (f): $f_{cPrOz,25\%}$:23% > $f_{cPrOz,50\%}$:20% > $f_{cPrOz,75\%}$:11% > $f_{cPrOz,90\%}$:8%. Moreover, for copolymers with higher initial cPrOz fractions, the monomer fraction in the polymer chain was found to be rather constant over the full course of polymerization. These differences in monomer fractions and distribution patterns are likely attributed to two factors: (i) reaction mixtures with higher initial 2-oxazoline concentrations comprise a higher probability of 2-oxazoline-derived active chain ends, which can accelerate the propagation of 2-oxazine monomers, and (ii) reaction mixtures with lower initial 2-oxazine concentrations reveal a faster monomer consumption and, consequently, a more drastic drop in monomer concentration, which decreases the probability of a 2-oxazine addition to the active chain end during the kinetics. Derived from the monomer fractions, we calculated the reactivity ratios and propagation constants (Tables S2 and S3). In contrast to the homopolymerizations, cPrOx propagated about 20 times slower ($k_p = 11\ 10^{-3}$ L mol^{-1} s^{-1}; Figure S5), while the propagation of cPrOz was approximately 20 times faster ($k_p = 481\ 10^{-3}$ L mol^{-1} s^{-1}; Figure S5). Previous studies investigating the reactivity switch of 2-oxazoline and 2-oxazine monomers with different substituents in 2-position observed similar results (~25-fold increase for 2-oxazines and 15- to 20-fold decrease for 2-oxazolines) [22]. Due to the identical substituents used in this study, we assume that the values obtained in the current study represent a guideline for the estimation of reactivity switches and propagation changes for the copolymerization of 2-oxazolines and 2-oxazines with the same side chain chemistry. The obtained reactivity ratios ($r_{cPrOz} = 2.69$; $r_{cPrOx} = 0.40$) further confirmed the reactivity switch. Previous studies have reported the dependence of the reactivity ratios on the substituent in 2-position [21, 22]. Here, the dependence on the ring chemistry is reported, leading to gradient copolymers. Over the course of polymerization, all polymers furthermore revealed a linear increase in molar mass and monomodal monomer distributions (Figures S6 and S7), suggesting a controlled polymerization process.

3 | Thermal Characterization

One focal point of this work was the characterization of the thermal and solubility properties of PcPrOx$_{100}$ and PcPrOz$_{100}$ as well as their respective copolymers. Polymerizations were run to quantitative conversion to obtain polymers with an $X_n \approx 100$. The synthesized polymers were analyzed *via* ^{1}H NMR and SEC (Figures S8 and S9) and possessed the targeted monomer ratios and narrow dispersity. For evaluation of the effect of the X_n of PcPrOz, a homopolymer with 25 repeating units (PcPrOz$_{25}$; Figure S10) was also synthesized. The polymers were thermodynamically terminated using piperidine.

3.1 | Bulk Properties

To gain some insight into the bulk properties of the synthesized cPrOx and cPrOz, thermogravimetric analysis (TGA;

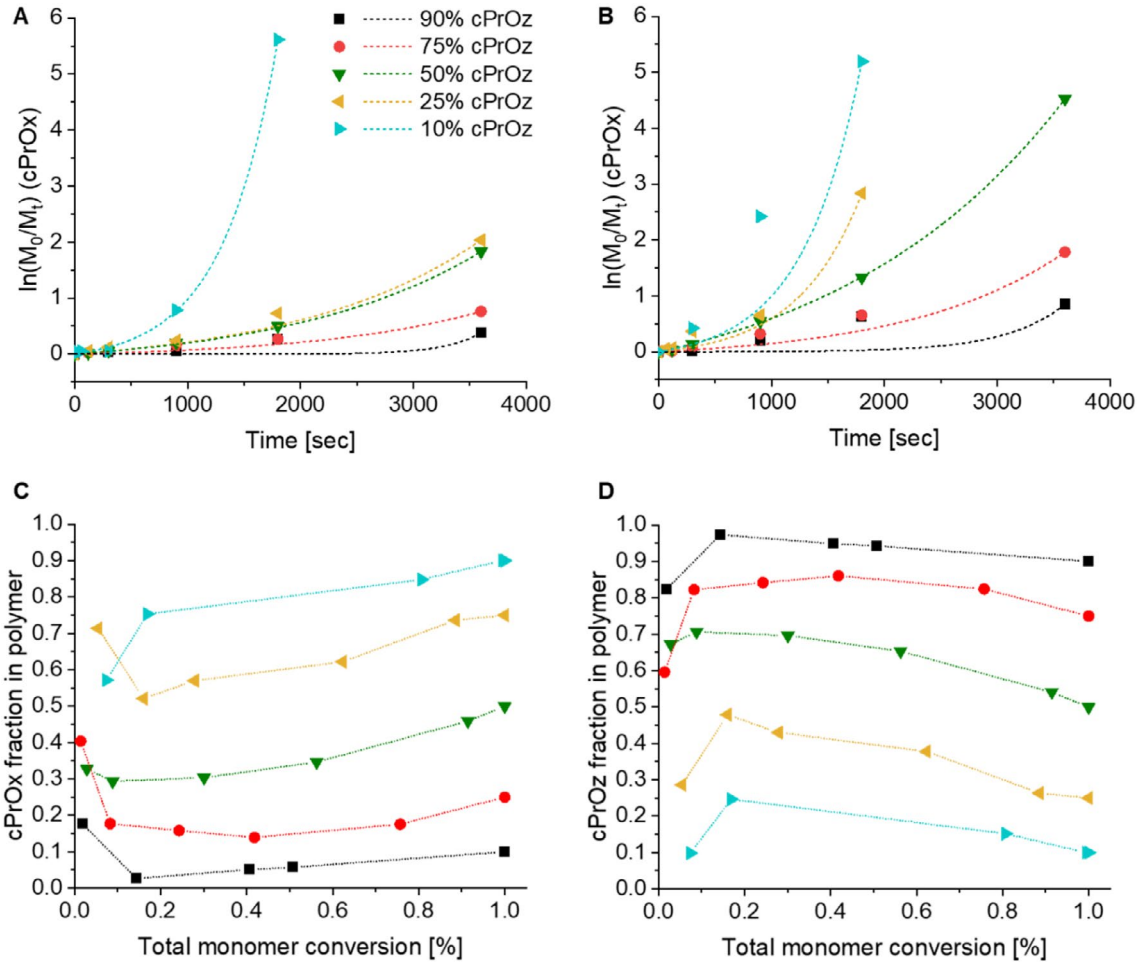

FIGURE 3 | Kinetic studies of the copolymerization of cPrOx and cPrOz at indicated monomer ratios. (A and B) kinetic plots and (C and D) conversion-dependent monomer fractions. $[M]/[I] = 100$; $M_0 = 2$ M; solvent: acetonitrile; initiator: MeOTos.

Figure S11, Table S4) and differential scanning calorimetry (DSC; Figure S12) were measured. With TGA, the degradation temperature was determined, whereas the glass transition temperature (T_g) was identified by DSC. Initial experiments were conducted with the homopolymers $PcPrOx_{100}$ and $PcPrOz_{100}$.

As for TGA measurements, the initial mass loss (2%–5% for $PcPrOx_{100}$ and ~2% for $PcPrOz_{100}$) at around 100°C indicated some residual solvent impurities. The residual solvent was most likely diethyl ether as it was used to precipitate the polymers during purification. A 10% mass loss was observed at 326°C for $PcPrOx_{100}$ and at 352°C for $PcPrOz_{100}$. A 50% mass loss was observed at 417°C for the $PcPrOx_{100}$—the value is ~10°C higher compared to the literature value of P(2-*n*-propyl-2-oxazoline) [44]—and at 421°C for $PcPrOz_{100}$. The mass loss between 10% and 50% can be attributed to the loss of the side chain. The mass losses of $PcPrOx_{100}$ were slightly shifted to lower temperatures compared to $PcPrOz_{100}$, which is most likely due to the higher molecular mass of the POz backbone, as the side chain is the same in both polymers. The residual masses were 10% for $PcPrOx_{100}$ and 2% for $PcPrOz_{100}$.

For DSC measurements, solvent-free samples are crucial. Therefore, the samples were tempered before the measurement to remove any potential solvent traces. Figure S12 shows the second heating cycle for the homopolymers and statistical heteropolymers formed. For $PcPrOx_{100}$ a T_g of 79°C (midpoint) was determined (Figure S11, Table S4). This is similar to the T_g of 79°C ($X_n = 38$) determined by Bloksma *et al.* [26] For $PcPrOz_{100}$ and $PcPrOz_{25}$, respectively, a T_g of 41°C (midpoint) and 38°C (midpoint) was determined (Figure S11, Table S4). This is in line with literature as the observed T_g of poly(2-alkyl-2-oxazoline)s is usually 30°C–40°C higher than the equivalent POz [45]. The same holds true for the shorter $PcPrOz_{25}$ variant since the obtained T_g value of 38°C is 37°C lower in comparison to the T_g value of $PcPrOx_{26}$ previously reported [46]. The difference in T_g can be explained with the flexibility of the backbone. Poly(2-alkyl-2-oxazine)s have higher flexibility in the backbone than poly(2-alkyl-2-oxazoline)s due to their additional methylene group [47]. The results described above for the homopolymers agree with the trends in T_g values for the copolymers (Figure S11, Table S4). For all three copolymers, the T_g value rises with decreasing oxazine content: $T_g = 52$°C for P($cPrOx_{25}$-*stat*-$cPrOz_{75}$) < $T_g = 57$°C for P($cPrOx_{50}$-*stat*-$cPrOz_{50}$) < $T_g = 68$°C for P($cPrOx_{75}$-*stat*-$cPrOz_{25}$).

No endotherm melting point was observed up to 200°C for all polymers, which means the polymers are amorphous. PcPrOx was previously reported to be an amorphous polymer. Therefore, it seems plausible that the POz equivalent is amorphous as well

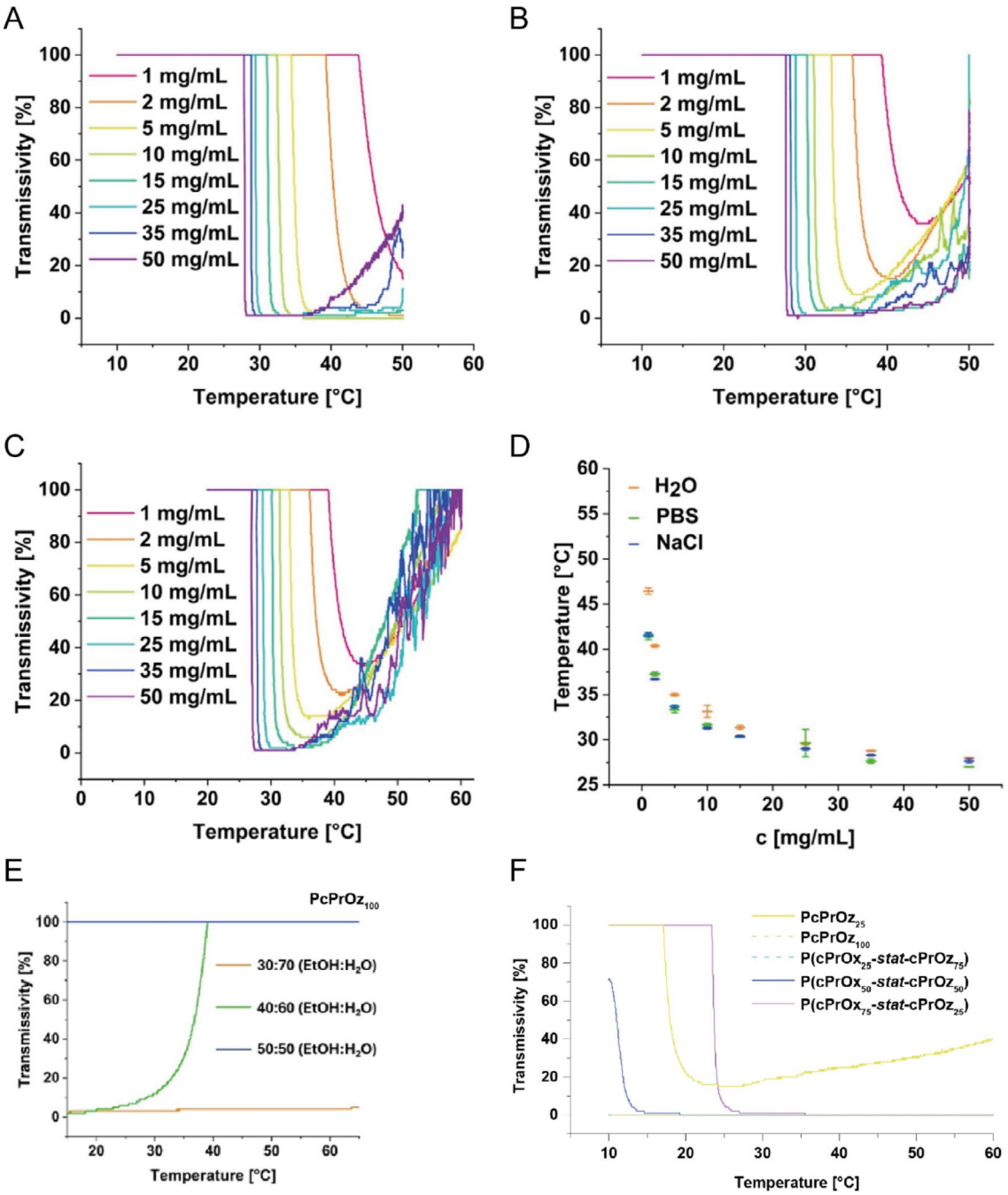

FIGURE 4 | Transmissivity for indicated PcPrOx concentrations at different temperatures in different media: H_2O (A), NaCl (0.9 wt%) (B), DPBS (C), and the respective T_{CP} with standard deviation (D; $n = 3$). (E) Temperature-dependent transmissivity for different solutions (EtOH:H_2O) of PcPrOz ($c = 5\,mg\,mL^{-1}$). (F) Transmissivity for indicated polymers at $c = 5\,mg\,mL^{-1}$ at different temperatures. Solvent: H_2O:EtOH (90:10).

[26]. To avoid (co)polymer degradation during DSC measurements, we only heated them to 200°C.

3.2 | Temperature-Dependent Solution Properties

Having possible future applications in biological systems in mind, the most relevant solvents are H_2O and aqueous buffers. Hence, turbidimetry measurements were carried out in H_2O, physiological (0.9 wt%) NaCl solution, and phosphate-buffered saline (PBS).

Figures 4 and S13–S15 show the turbidimetry results of $PcPrOx_{100}$, P(cPrOx$_{25}$-*stat*-cPrOz$_{75}$), P(cPrOx$_{50}$-*stat*-cPrOz$_{50}$), and P(cPrOx$_{75}$-*stat*-cPrOz$_{25}$). LCST behavior was observed in all three media since LCST behavior can be noticed by the distinct drop in transmissivity due to the precipitation of polymer. The temperature at which the transmissivity drops is lower for higher polymer concentrations, which is in line with literature reports [26]. However, we observed a concentration dependency for this effect as well: at higher temperatures, turbidity measurements for low polymer concentrations show, at first glance, a mixed behavior of LCST/UCST based on increasing

transmissivity values (> 0%) after a threshold. However, an explanation for this is not a mixed LCST/UCST property of the polymers. Indeed, $PcPrOx_{100}$ can be seen as a pseudo-peptide [48], and thus, it can be anticipated that the salting-in and salting-out effects of Hofmeister salts are similar for proteins and poly(2-oxazoline)s and show a pseudo-UCST behavior at higher temperatures. The used salts (NaCl, KCl, Na_2PO_4, and KH_2PO_4) are kosmotropic [49]. Hence, a salting-out effect (lowering the solubility) was observed for the LCST measurements in NaCl solution and PBS, not only for the homopolymer but also for the copolymers.

In water, the $PcPrOx_{100}$ sample with 1 mg mL^{-1} showed a minimum in transmissivity > 0% (Figure 4A), likely due to the low amount of precipitate. For NaCl, a minimum in transmissivity > 0% was observed for a polymer concentration up to 5 mg mL^{-1} (Figure 4B). For PBS, even the sample with 15 mg mL^{-1} showed a minimum in transmissivity > 0% (Figure 4C). These results nicely illustrate the salting-out effect in aqueous media. Moreover, the copolymer solubility decreased with rising 2-oxazine content or in other words, fewer copolymer concentrations were investigated for copolymer transmissivity studies in the various solvents compared to $PcPrOx_{100}$. For P($cPrOx_{75}$-*stat*-$cPrOz_{25}$), P($cPrOx_{50}$-*stat*-$cPrOz_{50}$), and P($cPrOx_{25}$-*stat*-$cPrOz_{75}$), the minimum transmissivity was reached for a concentration of 1 mg ml^{-1} in H_2O (Figures S13A, S14A, and S15A). Due to the raising copolymer hydrophobicity [50], the salting-out effect was enhanced by the kosmotropic salts, but only in the case of NaCl, shown by an increase of the minimum in transmissivity of 15 mg mL^{-1} for P($cPrOx_{50}$-*stat*-$cPrOz_{50}$) (Figure S14B) and P($cPrOx_{25}$-*stat*-$cPrOz_{75}$) (Figure S13B) compared to 5 mg mL^{-1} for $PcPrOx_{100}$ (Figure 4B) and P($cPrOx_{75}$-*stat*-$cPrOz_{25}$) (Figure S15B). However, we could not observe any difference in the transmissivity minimum with PBS (Figures S13C, S14C, and S15C) between the homopolymer and the copolymers (15 mg mL^{-1}). This might indicate that the salt concentration in PBS is already sufficient and therefore unable to further strengthen the salting-out effect (Figure 4C).

On the one hand, the minimum of transmissivity of the samples in salt solution is likely from the formation of larger aggregates due to salting-out effects. The aggregates accumulate and sediment to the bottom of the vial, and therefore the transmissivity drops no further. On the other hand, it might be a combination of LCST and UCST behavior based on complex thermal effects related to the copolymer interactions [34].

The difference between NaCl and PBS can be explained with the higher salt concentration of PBS (152 mM) versus NaCl (15.5 mM). For higher polymer concentrations, no minimum in transmissivity > 0% was observed because of the high amount of precipitate, and therefore the few aggregates formed by salting-out do not affect the transmissivity. The increase of transmissivity at higher temperatures is most likely due to the formation of larger aggregates that sediment to the bottom of the vial.

In theory the salting-out effect should translate to lower transmissivity for the same concentration in NaCl and PBS compared to water. In Figure 4D, T_{CP} (temperature at 50% transmissivity) for different concentrations in the three different media is shown. T_{CP} with increasing concentration shows nonlinear behavior. For the samples in the two salt solutions, the difference in T_{CP} was negligible despite the difference in salt concentrations. In comparison, the T_{CP} observed for water is higher up to 15 mg mL^{-1}. At higher concentrations ($c \geq 20$ mg mL^{-1}), the salt effect became negligible. So, at higher polymer concentrations salt in the used concentration seems to make no difference because the hydrophobic moieties outweigh the hydrophilic moieties with increasing temperature for LCST type polymers. The small decrease in T_{CP} from 35 to 50 mg mL^{-1} indicates the approaching of the LCST [26].

T_{CP} (5 mg mL^{-1} in H_2O, $X_n = 100$) for the three isomers poly(2-propyl-2-oxazoline)s was reported by Bloksma *et al.* [43]. Out of the three isomers, poly(2-*n*-propyl-2-oxazoline) showed the highest T_{CP} at 44°C, whereas poly(2-*iso*-propyl-2-oxazoline) showed the lowest T_{CP} at 27°C. $PcPrOx_{100}$, with a T_{CP} at 30°C, is in between [26]. The different T_{CP} can be explained by the different shielding of the hydrophilic moieties by the side chains. With a T_{CP} at 35°C under the same conditions, the synthesized $PcPrOx_{100}$ exhibited a slightly higher T_{CP} than the literature reference. The slight discrepancy in T_{CP} potentially resulted from different end groups slightly altering the polarity of the polymers [51].

The T_{CP} of the homopolymer hardly changes when the P($cPrOx_{75}$-*stat*-$cPrOz_{25}$) is tested in the three different solvents. However, the polymer concentration at which the T_{CP} is reached differs: For water, a T_{CP} is found at 25 mg mL^{-1} (29.9°C), whereas for PBS (29.8°C; $c = 5$ mg mL^{-1}) and NaCl (31.7°C; $c = 10$ mg mL^{-1}), the temperature-driven phase transition occurs at lower polymer concentrations (Figure S15D). This, in turn, might be attributable to the salting-out effect, which limits the solubility of the copolymers and favors their agglomeration [49]. This salting-out effect is negligible for the copolymers with increasing oxazine content (P($cPrOx_{50}$-*stat*-$cPrOz_{50}$)) since increased intermolecular interactions at higher polymer concentrations promote agglomeration [35]. As a result, the T_{CP} in water is achieved at 15 mg mL^{-1} (28.4°C), whereas in PBS (24.1°C; $c = 25$ mg mL^{-1}) and NaCl (27.9°C; $c = 25$ mg mL^{-1}), phase transition is only seen at higher polymer concentrations (Figure S14D). With P($cPrOx_{25}$-*stat*-$cPrOz_{75}$), the determination of T_{CP} values is difficult, as the limited solubility of the polymer provides hardly any data points for a T_{CP} analysis (Figure S13D).

Unlike $PcPrOx_{100}$, $PcPrOz_{100}$ was insoluble in water whereas it was soluble in EtOH. The isomers poly(2-*n*-propyl-2-oxazine) and poly(2-*iso*-propyl-2-oxazine) were previously reported to be soluble in water. Poly(2-*n*-propyl-2-oxazine) exhibited a LCST at 11°C (5 mg mL^{-1} in H_2O) [52]. The 2-oxazoline isomer of PcPrOz, poly(2-*n*-butyl-2-oxazoline), is reportedly insoluble in water but soluble in ethanol and features a UCST in water–ethanol mixtures containing 50–60 wt% ethanol [53]. The insolubility of $PcPrOz_{100}$ in water as compared to its POz isomers is probably rooted in the higher flexibility of the polymer backbone and the rigid side chain, resulting in shielding of the hydrophilic moieties and limiting its solubility in water.

Because $PcPrOz_{100}$ was found to be soluble in EtOH, its potential UCST in water–EtOH mixtures was studied. For this purpose, different EtOH–water mixtures (10:90; 30:70; 40:60; 50:50) of $PcPrOz_{100}$ ($c = 5\,mg\,mL^{-1}$) were studied with turbidimetry measurements ($T = 10°C–60°C$) (Figure 4E). While $PcPrOz_{100}$ remained soluble in the 50:50 mixture over the whole temperature range, the polymer was completely insoluble in the 10:90 and 30:70 mixtures. Solely for the 40:60 mixture, a UCST behavior was observed ($T_{CP} = 35°C$). The UCST behavior of $PcPrOz_{100}$ compared to the LCST behavior of $PcPrOx_{100}$ likely resulted from the higher hydrophobicity due to the additional methylene group in the backbone. Another explanation could be the high molar mass, as the dependency of T_{CP} on molar mass was previously reported for POx [54]. The latter aspect is consistent with the measurement data obtained for $PcPrOz_{25}$. Interestingly, the short homopolymers exhibited LCST behavior (EtOH:H_2O ratio of 10:90) (Figure 4F). Accordingly, the copolymers with the highest 2-oxazine content ($PrOx_{25}$-*stat*-$PrOz_{75}$) were insoluble in EtOH–water mixtures (90:10) and the increase of cPrOx within the copolymer structure resulted in improved solubility as indicated by their LCST behavior. As $PcPrOx_{100}$ itself was fully soluble in the applied media (data not shown), the observed T_{CP} is assumed to be fully attributed to the cPrOz fraction within the polymer chain.

4 | Conclusion

Here, we synthesized a novel cPrOz monomer for the formation of homopolymers with different chain lengths and the design of statistical copolymers including cPrOx. With the CROP strategy, we introduced the kinetics of nucleophilic cyclic imino ether attack on the terminal 2-oxazine or 2-oxazoline of the growing polymers. Our results demonstrate that the interaction with the polymeric five-membered ring system is favored in the homo- and cross-propagation, and the cPrOz monomers interact faster with the terminal polymeric cPrOx group compared to cPrOx monomers. The nucleophilic attack on the five-membered ring system is facilitated by its planarity and higher ring tension compared to the oxazines, resulting in reduced steric hindrance and enhanced interaction. Since the chain length of the homo- and heteropolymers is also controlled, tunable, temperature-responsive polymer characteristics are created. For example, the short-chain $PcPrOz_{25}$ possessed UCST properties, whereas the long-chain homopolymers $cPrOx_{100}$ and $cPrOz_{100}$ and heteropolymers showed LCST behavior. In other words, the smart combination of monomers allows the formation of statistical copolymers with controllable thermal polymer characteristics and identifies the potential of further monomer mixtures with resulting material properties. Based on those experimental results, understanding the kinetics of 2-oxazine and 2-oxazoline interactions during nucleophilic polymerization elongation provides a profound knowledge of the CROP mechanism and offers a strategy to form novel (co)polymers. In the future, the (co)polymers presented here will be investigated further regarding their properties as additives to tune the hydrophilicity of bulk materials in biofabrication and microplastics research. We will exploit their unique hydrophilic–hydrophobic balance to study their potential to increase hydrolytic degradation of materials, for example, by enzymes.

5 | Experimental Section

5.1 | Materials

2-Aminoethanol (>99%) and 3-amino-1-propanol (>99%) were purchased from TCI. Cyclopropyl cyanide (98%), piperidine (99.5%, extra dry), acetonitrile (99.9%, extra dry), and barium oxide (99.5%) were purchased from thermo scientific. Zinc acetate dihydrate (≥99%) was purchased from Carl Roth. Dichloromethane (DCM) (99.8%, analytical reagent grade) was purchased from Fisher Scientific. Deuterated chloroform ($CDCl_3$) (99.8%) was purchased from Deutero. Magnesium sulfate ($MgSO_4$) (99%, anhydrous) was purchased from Grüssing.

5.2 | NMR Spectroscopy

^{1}H- and ^{13}C-NMR spectra were acquired with a Bruker Avance III HD 500 MHz spectrometer or a Bruker Avance 300 MHz spectrometer. Some ^{1}H-NMR spectra for the kinetic samples were acquired with a Magritek Spinsolve 1.16.6 60 MHz spectrometer. Between each measurement, the spectrometer was shimmed with a shim sample (10% H_2O and 90% D_2O).

All spectra were calibrated *via* the residual solvent resonance of $CDCl_3$.

5.3 | Size-Exclusion Chromatography (SEC)

All polymers were analyzed with dimethylformamide-SEC (DMF-SEC) (sample solvent and eluent: DMF with lithium bromide (LiBr) ($5\,g\,L^{-1}$)) to determine $M_{n,app}$ and $Đ$. The measurements were conducted with a GRAM 10 µm 3000 Å gel column (separation range of 5000–5,000,000 Da) with a flow rate of $0.5\,mL\,min^{-1}$. For detection, a refractive index detector from Agilent Technologies (1260 Infinity series) was used. For calibration, a narrowly distributed polystyrene homopolymer (PSS calibration kit) was used. All samples were dissolved in eluent and filtered through a 0.22 µm polytetrafluoroethylene (PTFE) filter. Each measurement was performed with a 20 µL injection volume and toluene as an internal standard.

5.4 | Thermogravimetric Analysis (TGA)

TGA was performed on a Mettler TGA/DSC3. The measurements were conducted in aluminum oxide ceramic crucibles with a heating rate of $10\,K\,min^{-1}$ from 30°C to 700°C under a nitrogen atmosphere.

5.5 | Differential Scanning Calorimetry (DSC)

DSC was performed on a Mettler Toledo DSC 2 STARe system. Before measurement, the samples were tempered for 1 h at 100°C to remove residual solvent. The measurements were conducted in an aluminum pan with a pierced lid with a heating rate of $10\,K\,min^{-1}$ from 5°C to 220°C under a nitrogen atmosphere. The second heating cycle was used to determine T_m temperature and T_g.

5.6 | Turbidimetry

T_{CP} was measured on a Crystal16 parallel crystallizer turbidimeter developed by Avantium Technologies connected to a recirculation chiller and dry compressed air. Aqueous polymer solutions at indicated concentrations were heated and cooled at indicated temperature ranges (1.0°C min^{-1}). This cycle was repeated three times. The T_{CP} is reported as the 50% transmittance temperature in the second heating run.

Solutions (5 mg mL^{-1}) of polymer in a solvent mixture of EtOH and H_2O at indicated ratios were cooled and heated at indicated temperature ranges.

5.7 | Synthesis of 2-Cyclopropyl-2-Oxazoline (cPrOx)

The synthesis was adapted from a literature procedure [26, 41]. Cyclopropyl cyanide (670 mmol; 45.6 g; 1.0 equiv.) and ZnOAc (catalyst; 14 mmol; 3.0 g; 0.02 equiv.) were heated to 130°C. 2-Aminoethanol (750 mmol; 45.6 g; 1.1 equiv.) was added dropwise. After 22 h reaction time, the reaction mixture was cooled to room temperature. DCM was added and the organic phase was washed four times (3× with deionized H_2O and 1× with brine). The extracted solution was dried over $MgSO_4$ and filtered through a folded filter. Under reduced pressure, the DCM was removed (300 mbar). For further purification, the monomer was distilled under reduced pressure (46°C; 70 mbar) over barium oxide. After purification, the monomer was distilled dry *via* static distillation (70°C) over barium oxide.

^{1}H-NMR (500 MHz) in $CDCl_3$: $\delta = 4.17$ (2H, *t*, O—CH_2—CH_2), 3.78 (2H, *t*, N—CH_2—CH_2), 1.62 (1H, *m*, C—CH—$(CH_2)_2$), 0.87 (4H, *m*, CH—$(CH_2)_2$) ppm.

5.8 | Synthesis of 2-Cyclopropyl-2-Oxazine (cPrOz)

The synthesis was adapted from a literature procedure [41]. Cyclopropyl cyanide (680 mmol; 45.6 g; 1.0 equiv.) and ZnOAc (catalyst; 14 mmol; 3.0 g; 0.02 equiv.) were heated to 130°C. 3-Amino-1-propanol (750 mmol; 56.1 g; 1.1 equiv.) was added dropwise. After 22 h reaction time, the reaction mixture was cooled to room temperature. DCM (100 mL) was added, and the organic phase was washed four times (3× with deionized H_2O and 1× with brine; ~150 mL). The extracted solution was dried over $MgSO_4$ and filtered through a folded filter. Under reduced pressure, the DCM was removed (300 mbar). For further purification, the monomer was distilled under reduced pressure (90°C; 36 mbar) over barium oxide. After purification, the monomer was distilled dry under reduced pressure (80°C) over barium oxide.

Yield: 20 g (0.16 mol) colorless liquid; 23.5%.

^{1}H-NMR (500 MHz) in $CDCl_3$: $\delta = 4.09$ (2H, *t*, O—CH_2—CH_2), 3.30 (2H, *t*, N—CH_2—CH_2), 1.81 (2H, quint., CH_2—CH_2—CH_2), 1.40 (1H, *m*, C—CH—$(CH_2)_2$), 0.87 (4H, *m*, CH—$(CH_2)_2$) ppm.

^{13}C-NMR (125 MHz) in $CDCl_3$: $\delta = 65$ (O—CH_2—CH_2), 42 (2H, *t*, N—CH_2—CH_2), 22 (CH_2—CH_2—CH_2), 14 (C—CH—$(CH_2)_2$), 5 (CH—$(CH_2)_2$) ppm.

5.9 | Microwave-Assisted Polymerizations

All kinetics and polymerizations were conducted using a Biotage Initiator Eight+ microwave. All reactions were carried out in sealed containers with the "organic synthesis" mode.

5.10 | Kinetic Study of the Homopolymerization of 2-Cyclopropyl-2-Oxazoline

Five milliliters of stock solution with an initial cPrOx concentration of 2 M (10 mmol; 1.1 g) and a ratio of [cPrOx]/[MeOTos] = 100 (MeOTos: 0.1 mmol; 0.019 g) in 3.9 mL acetonitrile was prepared under Ar atmosphere. Under Ar, the stock solution was divided over nine microwave vials (0.4 mL per vial). The vials were closed with a crimped septum. One vial was held back for reference. Each of the eight remaining vials had a different reaction time at 140°C reaction temperature in the microwave synthesizer (1 s; 30 s; 1 min; 2 min; 5 min; 10 min; 15 min; 30 min). The monomer conversion was determined *via* ^{1}H-NMR, comparing the signals at $\delta = 0.8$ ppm (4H, constant integral) and $\delta = 4.15$ ppm, which decreased over the course of the polymerization.

5.11 | Kinetic Study of the Homopolymerization of 2-Cyclopropyl-2-Oxazine

Five milliliters of stock solution with an initial cPrOz concentration of 2 M (10 mmol; 1.3 g) and a ratio of [cPrOz]/[MeOTos] = 100 (MeOTOs: 0.1 mmol; 0.019 g) in 3.7 mL acetonitrile was prepared under Ar atmosphere. Under Ar, the stock solution was divided over nine microwave vials (0.4 mL per vial). The vials were closed with a crimped septum. One vial was held back for reference. Each of the eight remaining vials had a different reaction time at a 140°C reaction temperature in the microwave synthesizer (1 s; 60 s; 1 min; 3 min; 5 min; 10 min; 15 min; 30 min; 60 min). The monomer conversion was determined *via* ^{1}H-NMR by comparing the signals at $\delta = 0.8$ ppm (4H, constant integral) and $\delta = 4.1$ ppm, which decreases over the course of the polymerization.

5.12 | Copolymerization Kinetics

Copolymerization kinetics were conducted according to the homopolymerization kinetics described above. For monomer ratios, please refer to Table S5.

The polymer composition (F) was determined by ^{1}H NMR spectroscopy from the monomer conversion (Tables S1 and S2). The copolymerization parameters r_{cPrOz} and r_{cPrOx} were calculated using Equations (1) and (2) (for the explanation of terms, see footnote of Table S2).

$$F_1 = \frac{r_1 f_1^2 + f_1 f_2}{r_1 f_1^2 + 2 f_1 f_2 + r_2 f_2^2} \quad (1)$$

$$\eta = \left(r_1 + \left(\frac{r_2}{\alpha}\right)\right)\xi\left(\frac{r_2}{\alpha}\right) \quad (2)$$

5.13 | Polymer Synthesis

The kinetics were calculated to 98% monomer conversion with k_p that was determined with the kinetic studies. The polymerization and purification procedure is exemplarily described for the synthesis of $PcPrOx_{100}$. For all other polymers, please refer to Table S5.

5.14 | Synthesis of Poly(2-Cyclopropyl-2-Oxazoline) (PcPrOx)

Twenty milliliters of reaction mixture with an initial cPrOx concentration of 2 M (40 mmol; 4.5 g) and a ratio of [cPrOx]/[MeOTos] = 100 (MeOTos: 0.4 mmol; 0.075 g) in 15.5 mL acetonitrile was prepared in a microwave vial under Ar atmosphere. The reaction was carried out at 140°C in the microwave synthesizer with a reaction time of 14 min 10 s. After the reaction time, 1 mL of sample was taken for calculation of conversion. The polymer was terminated with 5.0 equiv. piperidine relative to the initiator (2 mmol; 0.17 g). After the piperidine addition, the mixture was stirred overnight at 40°C. For purification, the polymer was precipitated in 240 mL diethyl ether (−80°C). After centrifugation at 5000 rpm for 3 min, the supernatant was discarded, and the residue was dissolved in 10 mL DCM. The polymer solution was precipitated in 140 mL diethyl ether and centrifuged at 5000 rpm for 3 min. The supernatant was discarded, and the purified polymer was dried in the vacuum oven at 40°C overnight.

Yield: 3.59 g (X_n = 100).

^{1}H-NMR (500 MHz) in $CDCl_3$: δ = 3.5 (4H, br, O—CH_2—CH_2—N), 1.6 (1H, br, C—CH—$(CH_2)_2$), 0.9 (4H, *m*, CH—$(CH_2)_2$) ppm.

SEC (DMF, PS-cal.): $M_{n,app}$ = 4900 g mol^{-1}; $Đ$ = 1.39.

5.15 | Synthesis of Poly(2-Cyclopropyl-2-Oxazine) (PcPrOz)

Yield: 2.07 g (X_n = 90).

^{1}H-NMR (500 MHz) in $CDCl_3$: δ = 3.3 (4H, br, O—CH_2—CH_2—N), 1.5 (3H, br, CH_2—CH_2—CH_2, C—CH—$(CH_2)_2$), 0.75 (4H, br, CH—$(CH_2)_2$) ppm.

SEC (DMF, PS-cal.): $M_{n,app}$ = 10,800 g mol^{-1}; $Đ$ = 1.59.

Acknowledgments

The authors would like to thank Rika Schneider for SEC measurements. The authors thank the German Research Foundation (DFG; Collaborative Research Center SFB/TRR225 "From the fundamentals of Biofabrication to functional tissue models")—project number 326998133 for financial support. T.M.L. thanks the German Research Foundation (DFG; Collaborative Research Center SFB1357 Microplastic)—project number 391977956.

Conflicts of Interest

The authors declare no conflicts of interest.

Data Availability Statement

The primary data are available. The supporting information is available free of charge and contains further analysis of the materials in this study, including NMR spectra, SEC data, turbidimetry data as well as TGA and DSC results.

References

1. R. Hoogenboom, "The Future of Poly(2-Oxazoline)s," *European Polymer Journal* 179 (2022): 111521, https://doi.org/10.1016/j.eurpolymj.2022.111521.

2. T. Lorson, M. M. Lübtow, E. Wegener, et al., "Poly(2-Oxazoline)s Based Biomaterials: A Comprehensive and Critical Update," *Biomaterials* 178 (2018): 204–280, https://doi.org/10.1016/j.biomaterials.2018.05.022.

3. R. Luxenhofer, Y. Han, A. Schulz, et al., "Poly(2-Oxazoline)s as Polymer Therapeutics," *Macromolecular Rapid Communications* 33, no. 19 (2012): 1613–1631, https://doi.org/10.1002/marc.201200354.

4. K. Kempe, "Chain and Step Growth Polymerizations of Cyclic Imino Ethers: From Poly(2-Oxazoline)s to Poly(Ester Amide)s," *Macromolecular Chemistry and Physics* 218, no. 11 (2017): 1700021, https://doi.org/10.1002/macp.201700021.

5. T. G. Bassiri, A. Levy, and M. Litt, "Polymerization of Cyclic Imino Ethers. I. Oxazolines," *Journal of Polymer Science. Part B: Polymer Letters* 5, no. 9 (1967): 871–879, https://doi.org/10.1002/pol.1967.110050927.

6. T. Kagiya, S. Narisawa, T. Maeda, and K. Fukui, "Ring-Opening Polymerization of 2-Substituted 2-Oxazolines," *Journal of Polymer Science. Part B: Polymer Physics* 4, no. 7 (1966): 441–445, https://doi.org/10.1002/pol.1966.110040701.

7. W. Seeliger, E. Aufderhaar, W. Diepers, et al., "Recent Syntheses and Reactions of Cyclic Imidic Esters," *Angewandte Chemie International Edition in English* 5, no. 10 (1966): 875–888, https://doi.org/10.1002/anie.196608751.

8. D. A. Tomalia and D. P. Sheetz, "Homopolymerization of 2-Alkyl- and 2-Aryl-2-Oxazolines," *Journal of Polymer Science Part A-1: Polymer Chemistry* 4, no. 9 (1966): 2253–2265, https://doi.org/10.1002/pol.1966.150040919.

9. M. Hartlieb, K. Kempe, and U. S. Schubert, "Covalently Cross-Linked Poly(2-Oxazoline) Materials for Biomedical Applications—From Hydrogels to Self-Assembled and Templated Structures," *Journal of Materials Chemistry B* 3, no. 4 (2015): 526–538, https://doi.org/10.1039/C4TB01660B.

10. M. N. Leiske, "Poly(2-Oxazoline)-Derived Star-Shaped Polymers as Potential Materials for Biomedical Applications: A Review," *European Polymer Journal* 185 (2023): 111832, https://doi.org/10.1016/j.eurpolymj.2023.111832.

11. D. Pizzi, J. Humphries, J. P. Morrow, et al., "Poly(2-Oxazoline) Macromonomers as Building Blocks for Functional and Biocompatible Polymer Architectures," *European Polymer Journal* 121 (2019): 109258, https://doi.org/10.1016/j.eurpolymj.2019.109258.

12. P. Wilson, P. C. Ke, T. P. Davis, and K. Kempe, "Poly(2-Oxazoline)-Based Micro- and Nanoparticles: A Review," *European Polymer Journal* 88 (2017): 486–515, https://doi.org/10.1016/j.eurpolymj.2016.09.011.

13. V. P. Beyer, B. Cattoz, A. Strong, A. Schwarz, and C. R. Becer, "Brush Copolymers From 2-Oxazoline and Acrylic Monomers via an Inimer Approach," *Macromolecules* 53, no. 8 (2020): 2950–2958, https://doi.org/10.1021/acs.macromol.0c00243.

14. G. Delaittre, "Telechelic Poly(2-Oxazoline)s," *European Polymer Journal* 121 (2019): 109281, https://doi.org/10.1016/j.eurpolymj.2019.109281.

15. M. Glassner, M. Vergaelen, and R. Hoogenboom, "Poly(2-Oxazoline)s: A Comprehensive Overview of Polymer Structures and Their Physical Properties," *Polymer International* 67, no. 1 (2018): 32–45, https://doi.org/10.1002/pi.5457.

16. B. Guillerm, S. Monge, V. Lapinte, and J.-J. Robin, "How to Modulate the Chemical Structure of Polyoxazolines by Appropriate Functionalization," *Macromolecular Rapid Communications* 33, no. 19 (2012): 1600–1612, https://doi.org/10.1002/marc.201200266.

17. S. Jana and R. Hoogenboom, "Poly(2-Oxazoline)s: A Comprehensive Overview of Polymer Structures and Their Physical Properties—An Update," *Polymer International* 71, no. 8 (2022): 935–949, https://doi.org/10.1002/pi.6426.

18. B. Verbraeken, B. D. Monnery, K. Lava, and R. Hoogenboom, "The Chemistry of Poly(2-Oxazoline)s," *European Polymer Journal* 88 (2017): 451–469, https://doi.org/10.1016/j.eurpolymj.2016.11.016.

19. L. Loukotová, P. Švec, O. Groborz, et al., "Direct Comparison of Analogous Amphiphilic Gradient and Block Polyoxazolines," *Macromolecules* 54, no. 17 (2021): 8182–8194, https://doi.org/10.1021/acs.macromol.0c02674.

20. B. Verbraeken, J. Hullaert, J. van Guyse, K. Hecke, J. Winne, and R. Hoogenboom, "The Elusive Seven-Membered Cyclic Imino Ether Tetrahydrooxazepine," *Journal of the American Chemical Society* 140, no. 50 (2018): 17404–17408, https://doi.org/10.1021/jacs.8b10918.

21. M. R. Elzes, I. Mertens, O. Sedlacek, et al., "Linear Poly(Ethylenimine-Propylenimine) Random Copolymers for Gene Delivery: From Polymer Synthesis to Efficient Transfection With High Serum Tolerance," *Biomacromolecules* 23, no. 6 (2022): 2459–2470, https://doi.org/10.1021/acs.biomac.2c00210.

22. O. Sedlacek, K. Lava, B. Verbraeken, S. Kasmi, B. G. de Geest, and R. Hoogenboom, "Unexpected Reactivity Switch in the Statistical Copolymerization of 2-Oxazolines and 2-Oxazines Enabling the One-Step Synthesis of Amphiphilic Gradient Copolymers," *Journal of the American Chemical Society* 141, no. 24 (2019): 9617–9622, https://doi.org/10.1021/jacs.9b02607.

23. T. Saegusa, S. Kobayashi, and Y. Nagura, "Isomerization Polymerization of 1,3-Oxazine. II. Kinetic Studies of the Ring-Opening Isomerization Polymerization of Unsubstituted 5,6-Dihydro-4H-1,3,-Oxazine," *Macromolecules* 7, no. 3 (1974): 265–272.

24. G. Pasparakis and C. Tsitsilianis, "LCST Polymers: Thermoresponsive Nanostructured Assemblies Towards Bioapplications," *Polymer* 211 (2020): 123146, https://doi.org/10.1016/j.polymer.2020.123146.

25. R. Hoogenboom, H. M. L. Thijs, M. J. H. C. Jochems, B. M. van Lankvelt, M. W. M. Fijten, and U. S. Schubert, "Tuning the LCST of Poly(2-Oxazoline)s by Varying Composition and Molecular Weight: Alternatives to Poly(*N*-Isopropylacrylamide)?," *Chemical Communications* 44 (2008): 5758–5760, https://doi.org/10.1039/b813140f.

26. M. M. Bloksma, C. Weber, I. Y. Perevyazko, et al., "Poly(2-Cyclopropyl-2-Oxazoline): From Rate Acceleration by Cyclopropyl to Thermoresponsive Properties," *Macromolecules* 44, no. 11 (2011): 4057–4064, https://doi.org/10.1021/ma200514n.

27. N. M. Warne, J. R. Finnegan, O. M. Feeney, and K. Kempe, "Using 2-Isopropyl-2-Oxazine to Explore the Effect of Monomer Distribution and Polymer Architecture on the Thermoresponsive Behavior of Copolymers," *Journal of Polymer Science* 59, no. 22 (2021): 2783–2796, https://doi.org/10.1002/pol.20210551.

28. S. Abbrent, A. Mahun, M. D. Smrčková, et al., "Copolymer Chain Formation of 2-Oxazolines by In Situ 1H-NMR Spectroscopy: Dependence of Sequential Composition on Substituent Structure and Monomer Ratios," *RSC Advances* 11, no. 18 (2021): 10468–10478, https://doi.org/10.1039/D1RA01509E.

29. M. Glassner, K. Lava, V. R. de La Rosa, and R. Hoogenboom, "Tuning the LCST of Poly(2-Cyclopropyl-2-Oxazoline) via Gradient Copolymerization With 2-Ethyl-2-Oxazoline," *Journal of Polymer Science Part A: Polymer Chemistry* 52, no. 21 (2014): 3118–3122, https://doi.org/10.1002/pola.27364.

30. M. N. Leiske, R. Singha, S. Jana, B. G. de Geest, and R. Hoogenboom, "Amidation of Methyl Ester-Functionalised Poly(2-Oxazoline)s as a Powerful Tool to Create Dual pH- and Temperature-Responsive Polymers as Potential Drug Delivery Systems," *Polymer Chemistry* 14 (2023): 2034–2044, https://doi.org/10.1039/D3PY00050H.

31. Z. A. I. Mazrad, B. Schelle, J. A. Nicolazzo, M. N. Leiske, and K. Kempe, "Nitrile-Functionalized Poly(2-Oxazoline)s as a Versatile Platform for the Development of Polymer Therapeutics," *Biomacromolecules* 22, no. 11 (2021): 4618–4632, https://doi.org/10.1021/acs.biomac.1c00923.

32. Z. Varanaraja, N. Hollingsworth, R. Green, and C. R. Becer, "Poly(2-Alkyl-2-Oxazoline)-Based Copolymer Library With a Thermoresponsive Behavior in Dodecane," *ACS Applied Polymer Materials* 5, no. 7 (2023): 5158–5168, https://doi.org/10.1021/acsapm.3c00625.

33. V. Mair, I. Paulus, J. Groll, and M. Ryma, "Freeform Printing of Thermoresponsive Poly(2-Cyclopropyl-Oxazoline) as Cytocompatible and On-Demand Dissolving Template of Hollow Channel Networks in Cell-Laden Hydrogels," *Biofabrication* 14, no. 2 (2022): 025019, https://doi.org/10.1088/1758-5090/ac57a7.

34. J. Seuring and S. Agarwal, "Polymers With Upper Critical Solution Temperature in Aqueous Solution," *Macromolecular Rapid Communications* 33, no. 22 (2012): 1898–1920, https://doi.org/10.1002/marc.201200433.

35. Q. Zhang and R. Hoogenboom, "Polymers With Upper Critical Solution Temperature Behavior in Alcohol/Water Solvent Mixtures," *Progress in Polymer Science* 48 (2015): 122–142, https://doi.org/10.1016/j.progpolymsci.2015.02.003.

36. R. Hoogenboom and H. Schlaad, "Thermoresponsive Poly(2-Oxazoline)s, Polypeptoids, and Polypeptides," *Polymer Chemistry* 8, no. 1 (2017): 24–40, https://doi.org/10.1039/C6PY01320A.

37. M. M. Bloksma, D. J. Bakker, C. Weber, R. Hoogenboom, and U. S. Schubert, "The Effect of Hofmeister Salts on the LCST Transition of Poly(2-Oxazoline)s With Varying Hydrophilicity," *Macromolecular Rapid Communications* 31, no. 8 (2010): 724–728, https://doi.org/10.1002/marc.200900843.

38. S. Jana and M. Uchman, "Poly(2-Oxazoline)-Based Stimulus-Responsive (Co)Polymers: An Overview of Their Design, Solution Properties, Surface-Chemistries and Applications," *Progress in Polymer Science* 106 (2020): 101252, https://doi.org/10.1016/j.progpolymsci.2020.101252.

39. L. Liu, M. Xu, Y. Ye, and B. Zhang, "On the Degradation of (Micro)Plastics: Degradation Methods, Influencing Factors, Environmental Impacts," *Science of the Total Environment* 806 (2022): 151312, https://doi.org/10.1016/j.scitotenv.2021.151312.

40. A. R. Othman, H. A. Hasan, M. H. Muhamad, N. Ismail, and S. R. S. Abdullah, "Microbial Degradation of Microplastics by Enzymatic Processes: A Review," *Environmental Chemistry Letters* 19, no. 4 (2021): 3057–3073, https://doi.org/10.1007/s10311-021-01197-9.

41. M. M. Lübtow, M. S. Haider, M. Kirsch, S. Klisch, and R. Luxenhofer, "Like Dissolves Like? A Comprehensive Evaluation of Partial Solubility Parameters to Predict Polymer–Drug Compatibility in Ultrahigh Drug-Loaded Polymer Micelles," *Biomacromolecules* 20, no. 8 (2019): 3041–3056, https://doi.org/10.1021/acs.biomac.9b00618.

42. H. Goossens, S. Catak, M. Glassner, et al., "Cationic Ring-Opening Polymerization of 2-Propyl-2-Oxazolines: Understanding Structural Effects on Polymerization Behavior Based on Molecular Modeling," *ACS Macro Letters* 2, no. 8 (2013): 651–654, https://doi.org/10.1021/mz400293y.

43. M. M. Bloksma, R. M. Paulus, H. P. C. van Kuringen, et al., "Thermoresponsive Poly(2-Oxazine)s," *Macromolecular Rapid Communications* 33, no. 1 (2012): 92–96, https://doi.org/10.1002/marc.201100587.

44. P. Bouten, K. Lava, J. van Hest, and R. Hoogenboom, "Thermal Properties of Methyl Ester-Containing Poly(2-Oxazoline)s," *Polymers* 7, no. 10 (2015): 1998–2008, https://doi.org/10.3390/polym7101494.

45. M. M. Bloksma, U. S. Schubert, and R. Hoogenboom, "Poly(Cyclic Imino Ether)s Beyond 2-Substituted-2-Oxazolines," *Macromolecular Rapid Communications* 32, no. 18 (2011): 1419–1441, https://doi.org/10.1002/marc.201100138.

46. N. Oleszko-Torbus, A. Utrata-Wesołek, M. Bochenek, D. Lipowska-Kur, A. Dworak, and W. Wałach, "Thermal and Crystalline Properties of Poly(2-Oxazoline)s," *Polymer Chemistry* 11, no. 1 (2020): 15–33, https://doi.org/10.1039/C9PY01316D.

47. Z. Varanaraja, J. Kim, and C. R. Becer, "Poly(2-Oxazine)s: A Comprehensive Overview of the Polymer Structures, Physical Properties and Applications," *European Polymer Journal* 147 (2021): 110299, https://doi.org/10.1016/j.eurpolymj.2021.110299.

48. R. Hoogenboom, "Poly(2-Oxazoline)s: A Polymer Class With Numerous Potential Applications," *Angewandte Chemie International Edition* 48, no. 43 (2009): 7978–7994, https://doi.org/10.1002/anie.200901607.

49. H. I. Okur, J. Hladílková, K. B. Rembert, et al., "Beyond the Hofmeister Series: Ion-Specific Effects on Proteins and Their Biological Functions," *Journal of Physical Chemistry B* 121, no. 9 (2017): 1997–2014, https://doi.org/10.1021/acs.jpcb.6b10797.

50. J. Mehringer, E. Hofmann, D. Touraud, S. Koltzenburg, M. Kellermeier, and W. Kunz, "Salting-In and Salting-Out Effects of Short Amphiphilic Molecules: A Balance Between Specific Ion Effects and Hydrophobicity," *Physical Chemistry Chemical Physics* 23, no. 2 (2021): 1381–1391, https://doi.org/10.1039/D0CP05491G.

51. S. Huber, N. Hutter, and R. Jordan, "Effect of End Group Polarity Upon the Lower Critical Solution Temperature of Poly(2-Isopropyl-2-Oxazoline)," *Colloid and Polymer Science* 286, no. 14 (2008): 1653–1661, https://doi.org/10.1007/s00396-008-1942-7.

52. B. Verbraeken, "The Reactivity of Cyclic Imino-Ethers Towards Cationic Ring-Opening (Co)Polymerization: 2-Oxazolines, 2-Oxazines and 2-Oxazepines," 2018, Public Defense.

53. H. M. L. Lambermont-Thijs, H. P. C. van Kuringen, J. P. W. Put, U. S. Schubert, and R. Hoogenboom, "Temperature Induced Solubility Transitions of Various Poly(2-Oxazoline)s in Ethanol-Water Solvent Mixtures," *Polymers* 2, no. 3 (2010): 188–199, https://doi.org/10.3390/polym2030188.

54. P. Lin, C. Clash, E. M. Pearce, T. K. Kwei, and M. A. Aponte, "Solubility and Miscibility of Poly(Ethyl Oxazoline)," *Journal of Polymer Science. Part B: Polymer Physics* 26, no. 3 (1988): 603–619, https://doi.org/10.1002/polb.1988.090260312.

Supporting Information

Additional supporting information can be found online in the Supporting Information section.